Kerjaschki et al.: lnvasion of intrametastatic lymphatic vessels propagates lymph node metastasis of human and mouse mammary carcinomas

Supplementary information

Content

Supplementary table 1a

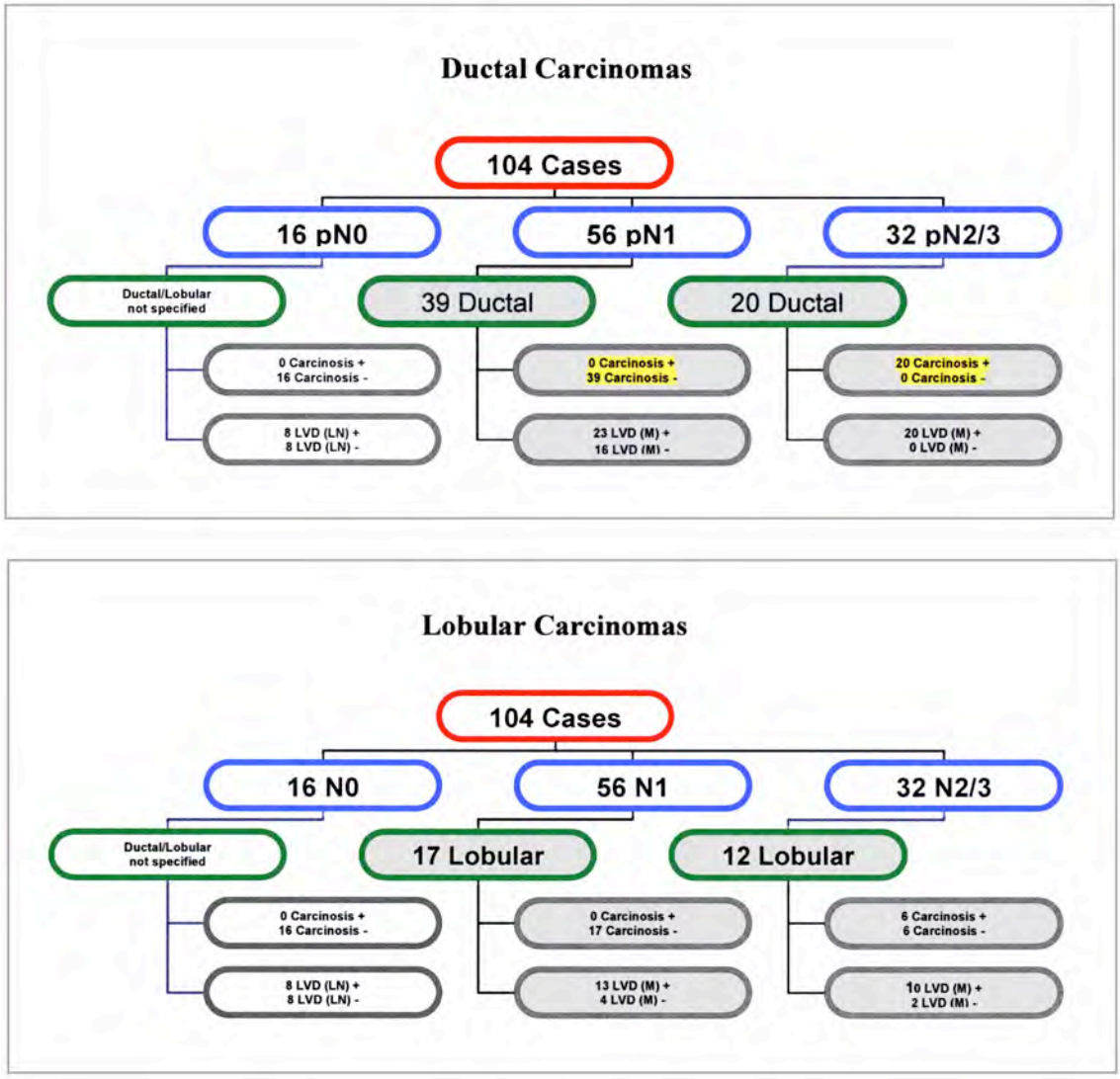

LVD	Lymphatic Vascular Density	**pN0:**	No regional lymph node metastasis
RLN	Residual Lymph Node	**N1:**	1-3 ipsilteral lymph nodes **(sentinel lymph node)**
M	Metastasis	**N2/3: metastases in**	post-sentinel lymph nodes
LN	Normal Lymph Node		

Listing of the patients and break down into histopathological groups and staging was performed according to the ***UICC*** *TNM Classification of Malignant Tumors, 7th edition (2009)*[12].

Supplementary table 1b
Receptor and p53 status

	Classification	**N**
Total number of cases		*104*
Estrogen receptor status	positive	79
	negative	24
	no data available	1
Progesteron receptor status	positive	55
	negative	49
	no data available	1
ERBB2 status*	not amplified	76
	amplified	28
p53 status	negative	78
	positive	26

*determined by immunohistochemistry and/or FISH

Supplementary table 2

Inhibitors used in the MCF7 spheroid/CCID assay

Arachidonic acid metabolism		**Target of Inhibitor**	**n**	**Reduction in CCID area** (+/- SD)	**p value**
Aspirin	100 µM 200 µM	COX1/2	11 12	0 0	- -
NS-398	20 µM	COX2	9	0	-
NDGA	25 µM 50 µM 75 µM	Pan-ALOX	10 16 16	51.1% (+/- 19.5) 62.8% (+/- 17.6) 88.3% (+/- 11.0)	0.0029 <0.0001 <0.0001
Caffeic acid	50 µM 100 µM 200 µM	ALOX5, ALOX15	11 10 12	0 0 52.4% (+/- 33.9)	- - 0.0024
Metalloproteases					
GM6001	10 µM 20 µM	Pan -MMP	10 10	23.3% (+/- 16.9) 25.1% (+/- 15.5)	n.s. 0.0481
TIMP1	100 ng/ml 200 ng/ml	Soluble MMPs	9 9	0 0	- -
TIMP2	100 ng/ml 200 ng/ml	Membrane-MMPs	9 10	0 26.7% (+/- 11.9)	- 0.0193
MMP2-Inhib II	10 µM 20 µM	MMP2	11 18	0 21.8% (+/- 19.7)	- 0.0258
MMP9-Inhib I	10 µM 20 µM	MMP9	12 15	0 26.2% (+/- 19.4)	- 0.0358
MMP13 Inh	10 µM 20 µM	MMP13	14 20	0 0	- -
Anti-MT1MMP-IgG 10µg/ml		MMP14	9	0	-
Aprotinin 1000U/ml		Non-MMP protease inhibitor	11	0	-
Radical scavengers					
Probucol 50 µM	50 µM 100 µM 200 µM	Lipid peroxidation, ROS	11 12 9	0 0 0	- - -
Mannitol 25 µM	25 µM 50 µM 100 µM	OH-radical	11 12 10	0 0 0	- - -
Catalase	300 U/ml 600 U/ml	H_2O_2 metabolism	12 11	0 0	- -
Carboxy-PTIO	100 µM 200 µM	NO-radical	10 9	0 0	- -

TIMP1 (CC1062), TIMP2 (CC3327), Polyclonal rabbit anti-MT1MMP antibody (AB8102; inhibitory antibody) were from Chemicon. GM6001, MMP2 inhibitor II, MMP9 inhibitor I, MMP13 (collagenase 3) inhibitor, and Carboxy-PTIO were from Calbiochem. Nordihydroguaiaretic acid (NDGA) was from Cayman Chemical. Aspirin, NS398, D-Mannitol, Catalase, Probucol, and Aprotinin were from Sigma. Caffeic acid was from Biomol. Statistical analysis was by paired t-test (significance p=0.05; SD=standard deviation). The paired two tailed t-test was used.

Supplementary figure 1
Lymphangiogenesis in residual lymph nodes and metastasis

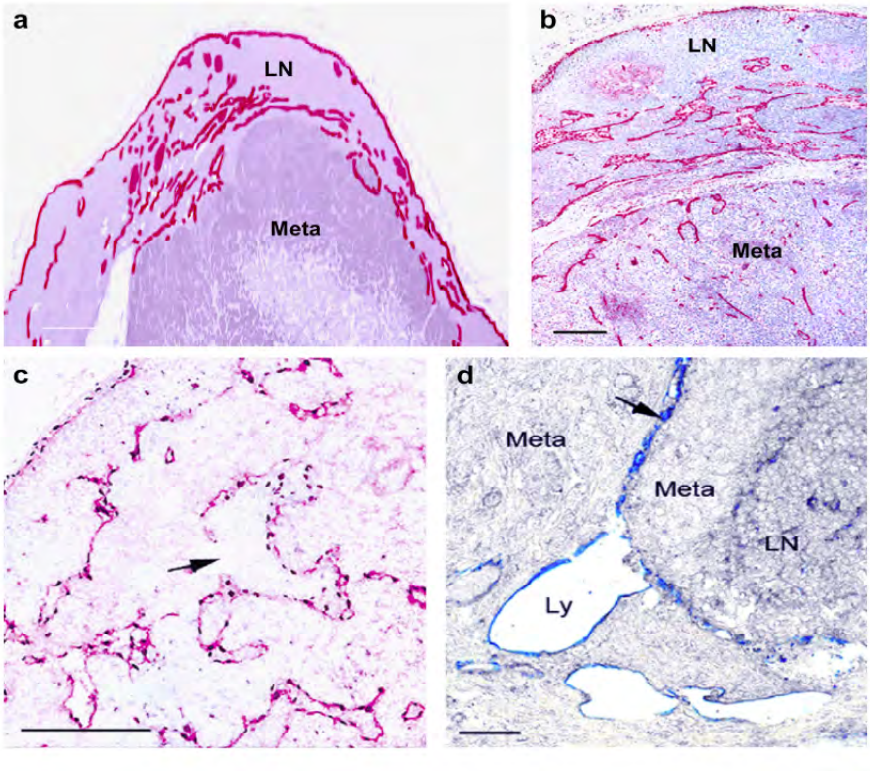

Lymphatic transformation of sentinel lymph node sinuses ("lymph node lymphangiogenesis") in the residual lymph node parenchyma and in sentinel metastases**. a,** lymphatic vessels (labeled with podoplanin, red) in a sentinel lymph node of a N1 ductal mammary carcinoma in which the intranodal lymphatics are restricted to the lymph node parenchyma (LN) and avoid the metastasis (Meta). **b**, lymphatic vessels (labeled with podoplanin, red) in a sentinel metastasis of a N2/3 ductal mammary carcinoma with lymphatic vessels both in the residual lymph node (LN) and within the metastasis (Meta). **c,** lymphatic vessels in a residual parenchyma of a sentinel lymph node of a N2/3 ductal mammary carcinoma. Lymphatic endothelial cells of extended vessels (arrow) are double labelled by podoplanin (red) and PROX1 (brown). **d**, continuity of an intrametastatic lymphatic vessel (blue, arrow) with a subcapsular lymph node sinus (Ly).

Scale bars: **a and d**, 200 µm; **b**, 100 µm; **c**, 10 µm.

Supplementary figure 2
MKI67^{+} endothelial cells in intrametastatic lymphatic endothelial cells

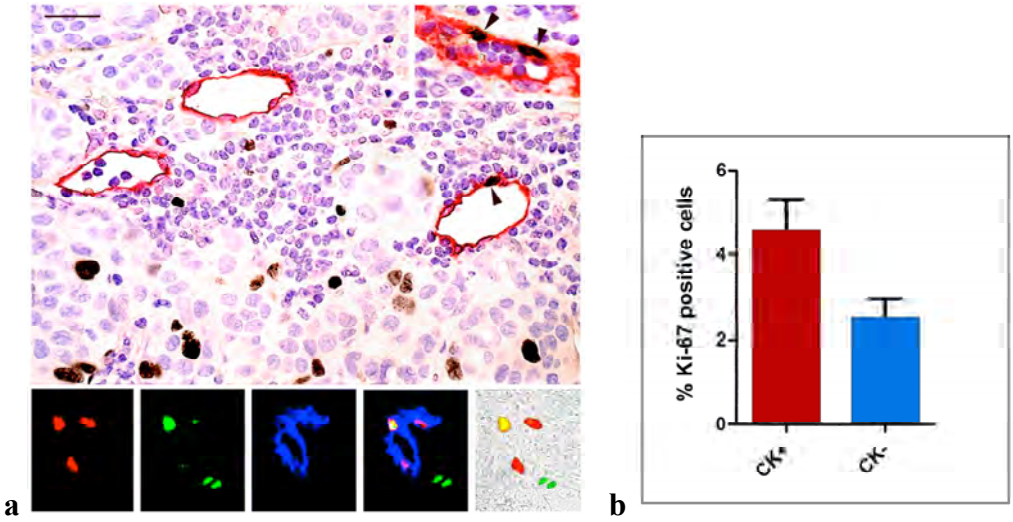

a. Sentinel metastasis of a ductal carcinoma with post-sentinel lymph node involvement, stage N2/3. Upper panel, MKI67 (Ki-67) is expressed in lymphatic endothelial cell nuclei (brown), and also in tumors cells. **Lower panels,** immunofluorescence using PROX1 (red), MKI67 (green) and podoplanin (blue) identifies single nuclei of lymphatic endothelial cells, as seen in the merged pictures at lower right.

Scale bar: 70 µm

b. Relative number of MKI67^{+} nuclei of lymphatic endothelial cells in intrametatstic lymphatic vessels containing emboli of cytokeratin^{+} tumors cells (CK^{+}, **red** column) and those devoid of luminal tumors cells (CK-, **blue** column) showing a significant ($p < 0.014$) difference. The results are derived from counting of 2929 nuclei of immunostained (MKI67, pan-cytokeratin and podoplanin) sentinel metastases of 5 cases of N2/3 ductal carcinomas.

Supplementary figure 3a
Expression of VEGFC in primary and metastatic ductal carcinomas

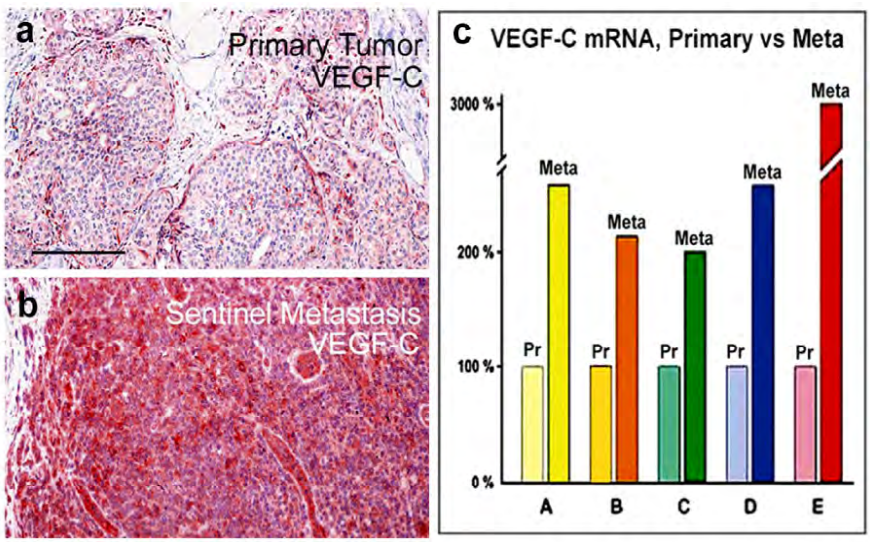

a and b, **Immunohistological localization of VEGFC** in a primary and sentinel metastatic ductal carinoma. The sections were processed in parallel, and reveal a uniform and significantly differential VEGFC expression. **c,** Real time PCR for expression of *VEGFC* mRNA in microdissected carcinoma cells of 5 selected patient's matched primary (Pr, light colours) and sentinel metastatic tumors (Meta, dark colours), revealing up to 30-fold overexpression in one of the metastases (case E).

Scale bar: 500 µm.

Supplementary figure 3b
Expression of VEGFA in primary an metastatic tumors

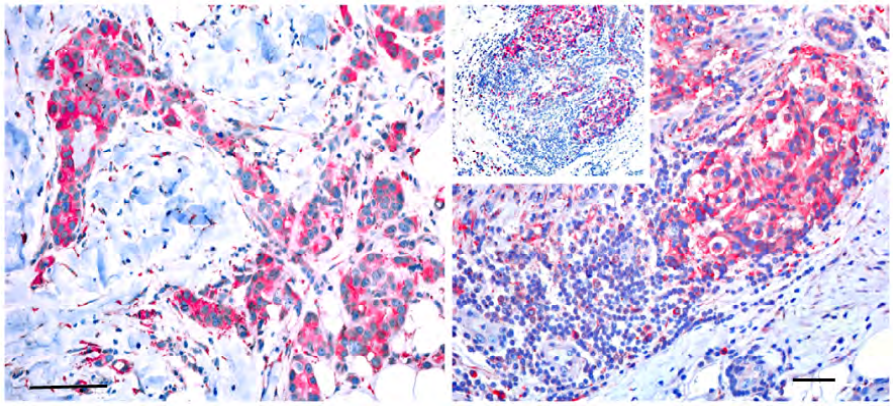

Immunohistological localization of VEGFA in a primary (left) and sentinel metastatic ductal carinoma (right) of patient E of Supplementary Figure 3a. The sections were processed in parallel and reveal no significant differences.

Scale bars: left, 100 µm, right, 500 µm.

Supplementary figure 3c
Expression of *VEGFA* mRNA in primary and metastatic tumors

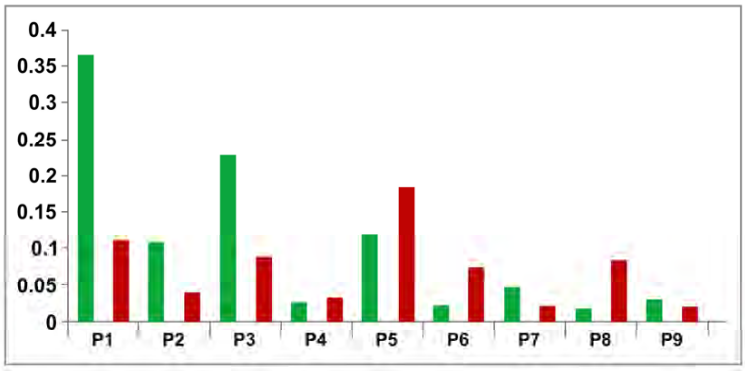

Real time PCR for expression of *VEGFA* mRNA in microdissected carcinoma cells of 9 selected patient's corresponding primary (green) and sentinel metastatic tumors (red), revealing a variable expression pattern. All cases were staged N2/3.

Methods for Supplementary figure 3

Microdissection and RNA isolation. Pure populations of ~10^4 – 10^5 tumors cells were isolated from hematoxylin/eosine stained frozen sections of primary tumors and lymph node metastases by laser-capture microdissection (LCM) with an Arcturus LCM instrument (Molecular Devices). Total RNA was isolated using TRIzol (Invitrogen) and further purified with the RNeasy Mini Kit (Qiagen). RNA quality was assessed using the Bioanalyser 2100 and the RNA 6000 pico LabChip Kit (Agilent, Palo Alto, CA).

RNA amplification and Affymetrix GeneChip hybridisation. Total RNA was subjected to two rounds of linear amplification via reverse transcription/*in vitro* transcription. 10µg of amplified cRNA were fragmented and hybridized to Affymetrix Human Genome U133A GeneChips. Washing, fluorescence staining, and scanning of the GeneChips were carried out according to the manufacturer's instructions.

Supplementary figure 4a
Differential gene expression in primary vs. metastatic carcinomas

Gene Name	Accs. Nr.	Symbol	fold	p
Regulator of G-protein signalling	NM_002922	*RGS1*	5.240	0.020
Dual specific phophatase	NM_004417	*DUSP1*	4.168	0.004
Cystine rich angiogenic inducer 61	NM_001554	*CYR61*	3.617	0.010
Chemokine (C-X-C) receptor 4	AF005058	*CXCR4*	3.597	0.055
Vascular endothelial growth factor C	NM_005429	*VEGFC*	1.590	0.099

Differential fold- expression of the above listed gene products was measured in metastases and primary breast tumors by oligoDNA microarrays (Affymetrix) of laser captured material. *VEGFC* was determined separately by real time PCR of microdissected tumors cells.

Supplementary figure 4b
Gene products that are diffentially expressed in primary vs. metastatic carcinomas

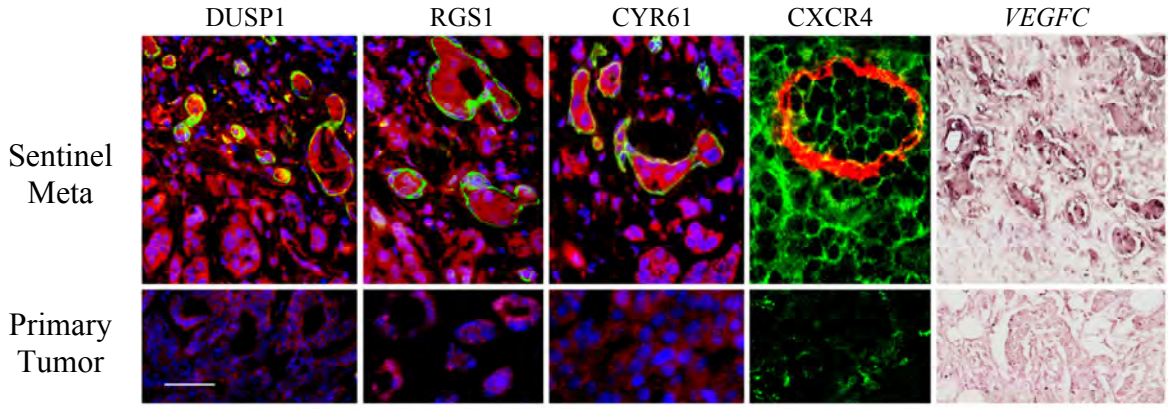

Enhanced expression of gene products listed in Supplememtary fig. 4a in **sentinel metastases** (**upper panels**) and lymphatic emboli, as compared to corresponding **primary tumors** (**lower panels**), revealed by immunofluorescenec with the respective antibodies (red), and podoplanin (green), or for *VEGFC* by *in situ* hybridization. For CXCR4 the coloration is reversed.

Scale bar: 50 µm.

Methods for Supplementary figure 4b

RNA was extracted from microdissected primary tumors and the corresponding sentinel lymphnode metastases of 24 breast cancer patients, twice amplified and profiled on Affimetrix U133A Chips,. For bioinformatic analysis microarray data were normalized using Robust Multi-Array Analysis as implemented in Bioconductor. All analyses were performed with log(2) transformed data. Differentially regulated genes in primary tumors vs. corresponding lymph node metastases were identified by modified t statistics with the Bioconductor LIMMA package. Genes were selected based on ≥2-fold changes in mean expression levels and p-values ≤ 0.01.

Smyth G, Limma K. Linear models for microarray data. In: Gentleman R, Carey V, Huber W, Irizarry R, Dudoit S. eds. *Bioinformatics and Computational Biology Solutions Using R and Bioconductor.* New York, USA: Springer; 2005:397-420

Supplementary figure 4c
Localization of gene products that are diffentially expressed in extrametastatic dermal and intrametastatic lymphatic vessels

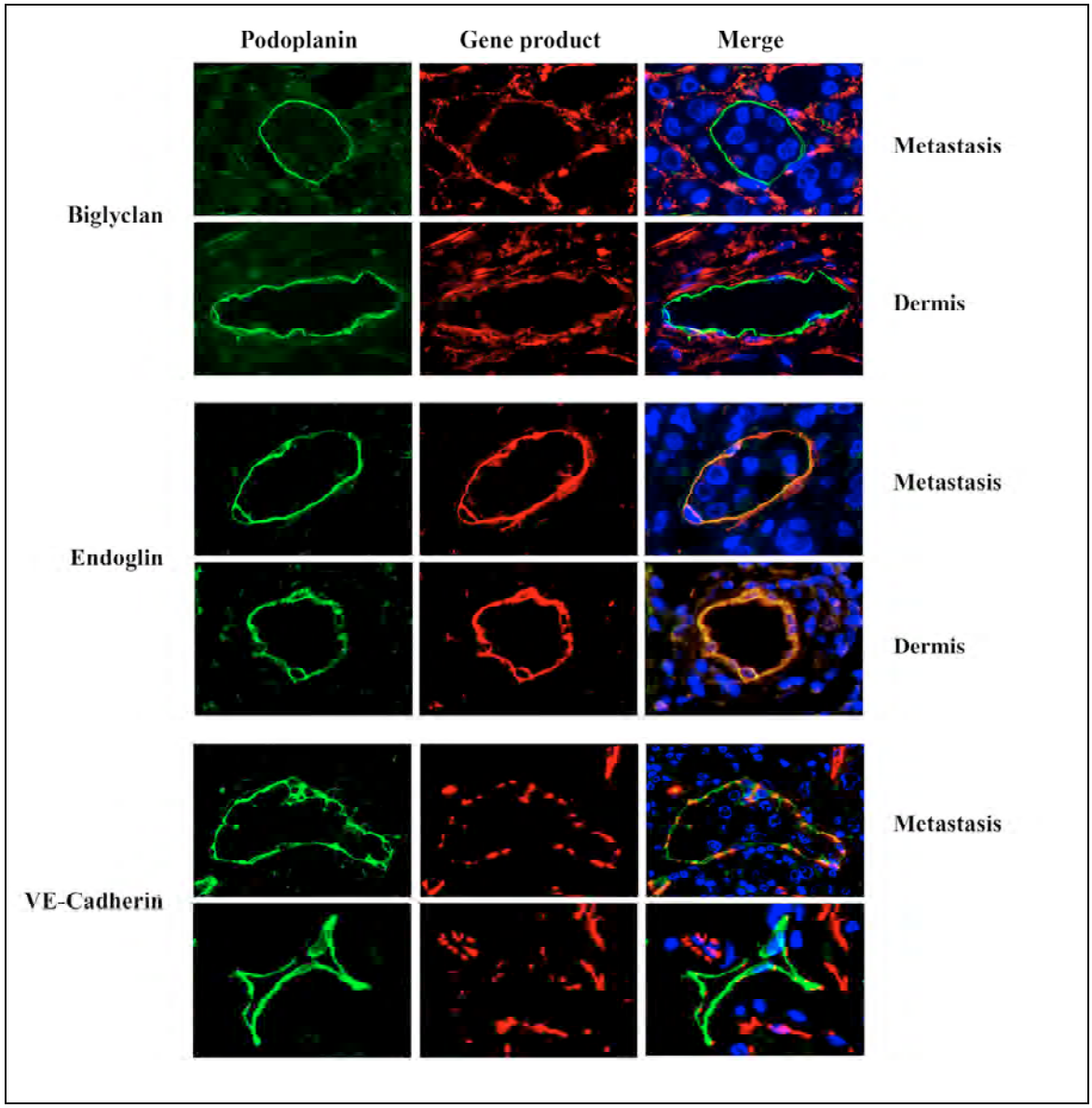

Colocalization of podoplanin^{+} lymphatic vessels **(green)** within the metastasis (upper panels in each box) and extrametastatic dermal lymphatics (lower panels in each box) with biglycan (*red*, upper box), endoglin (*red*, middle box) and VE-cadherin (*red,* lower box). The results indicate that there is no difference in the expression of these proteins in lymphatics of both groups. CD34 showed variable results (not shown).

Scale bar: 100 µm

Supplementary figure 5
Apoptosis of lymphatic endothelial cells in sentinel intrametastatic carcinosis

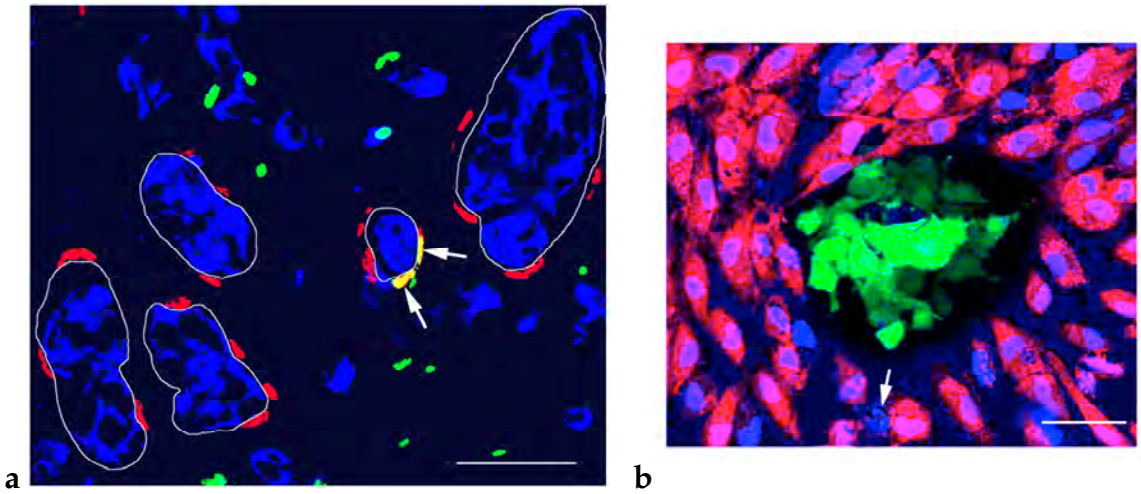

a. Localization of apoptotic lymphatic endothelial cells by triple immunofluorescence (**red:** PROX1, **blue:** pan-cytokeratin, **green:** TUNEL) in a paraffin section of sentinel intrametastatic carcinosis of a N2/3 carcinoma. Sporadic TUNEL and PROX1 double positive nuclei of lymphatic endothelial cells are indicated by arrows.

Scale bar: 15 µm

b. Apoptosis of lymphatic endothelial cells around MCF7 tumors cell spheroids. Confocal image of the base of a spheroid (made from MCF7 cells that stably express enhanced green fluorescent protein) forming a CCID in a monolayer of lymphatic endothelial cells (stably expressing red fluorescent protein), counterstained with Hoechst 33258 (blue). Endothelial nuclei are devoid of apoptotic nuclear fragmentation, there is only one single nuclear remnant of a sporadic apoptotic cell (white arrow). Co-incubation time was 4 h.

Scale bar: 50 µm

Supplementary figure 6
Toxcity of baicalein and 12(S)-HETE

a 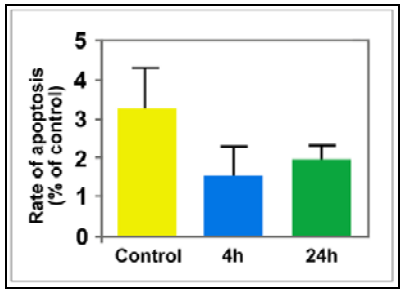

b 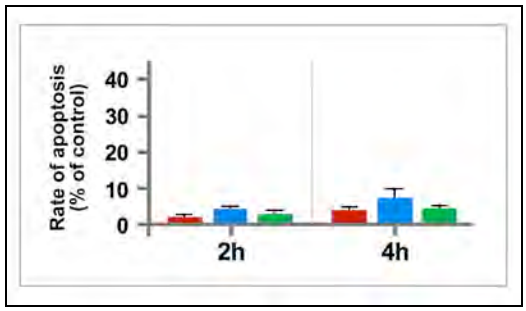

a. Baicalein is non-toxic to MCF7 cells. MCF7 cells were incubated with 100 µM baicalein for the indicated times and the percentage of apoptotic cells was measured by Hoechst 33258/propidium double staining of nuclei (performed in triplicate, n=250 nuclei/replicate). In the control group (yellow bar) 0.3 % ethanol (solvent for baicalein) was used.

b. Baicalein and 12(S)-HETE are non-toxic to lymphatic endothelial cells. Confluent lymphatic endothelial cells were incubated with 0.3 % ethanol solvent (red bars), 100µM baicalein (blue bars), or 1 µM 12(S)-HETE (green bars), for the indicated times. The percentage of apoptotic cells was measured by Hoechst 33258/propidium double staining of nuclei (performed in triplicate, n=250 nuclei/replicate).

Supplementary figure 7
Efficiency of the knock in of *ALOX12* cDNA in MCF7/*ALOX15* cells

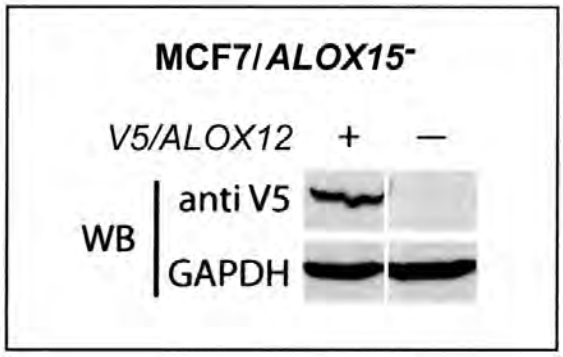

Protein expression of *ALOX12* - that is a priori not produced by MCF7 cells - was confirmed by Western blotting (WB) in MCF7/*ALOX15*$^{-}$ cells that were transfected with *ALOX12* cDNA fused to a *V5*-tag (*V5/12LOX*), or with a control vector.

Supplementary figure 8
ALOX gene expression in MCF7/*VEGFC* cells

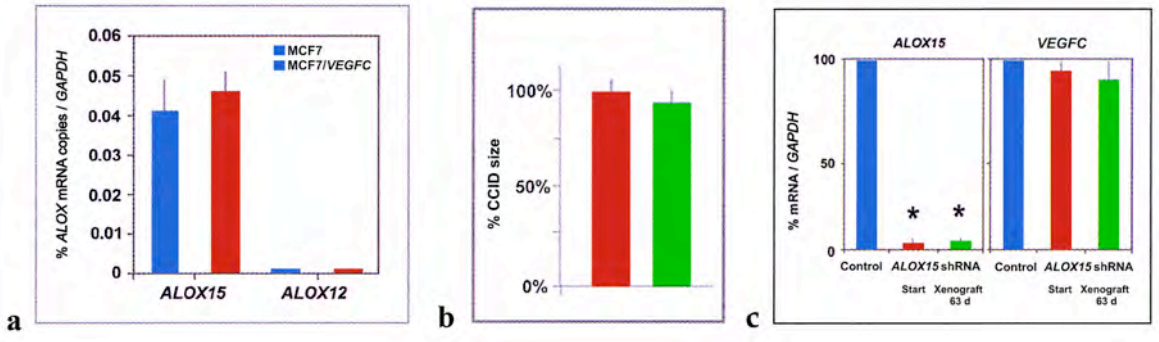

a. The expression of the *ALOX* genes, was similar in MCF7 cells with (red bar) or without (blue bar) *VEGFC* transgene expression. *ALOX12* was not expressed in any of the MCF7 variants. n = 3.

b. Transgene *VEFGC* overexpression in MCF7 clones did not reduce their CCID forming capacity. MCF7/*VEGFC* cells (red column) that were used throughout the knock down *in vivo* experiments induced similar CCIDs in lymphatic endothelial cells as MCF7 mock transfected controls (green column).

c. Stability of transgene expression in xenografted tumors cells. Xenograft tumors of MCF7/*VEGFC* cells excised after 63 days (**green bars**) maintained the shRNA mediated supression of *ALOX15* of 4.2% of controls ($p < 0.0001$), i.e. identical to that at the start of the experiments (2.4%, red bars; $p< 0.0001$). The transgene expression of *VEGFC* was also stable throughout the *in vivo* experiment. blue bars indicate mock controls; n= 3;

Supplementary figure 9
ALOX12 in sentinel lymph node metastasis

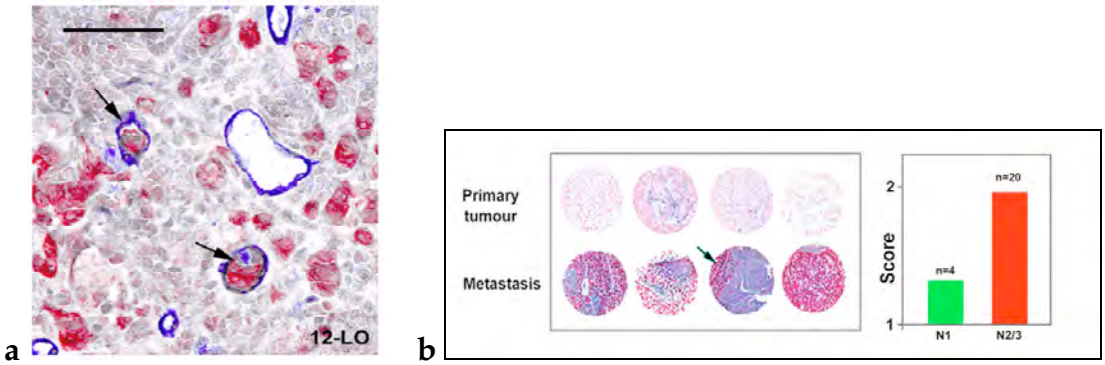

a. Sentinel metastasis of a ductal carcinoma with ALOX12 expressing tumor cells (**red**) that are located outside and inside of intrametastatic lymphatic vessels (**podoplanin: blue**).

Scale bar: 10 μm

b. Left: Samples from a tissue array containing punches of pT1c/pN1a ductal carcinomas. Primary tumors are in the upper lane, and were scored 0 for the expression of ALOX12, while their corresponding sentinel metastases in the lower lane were scored 2. Immunostaining (**red**) is for ALOX12. Occasionally only a small segment of the punch contains tumors (arrow). **Right:** Cumulative scores for ALOX12 expression in 24 ductal carcinomas. Scoring was performed by two independent observers. **N1** indicates metastasis in the sentinel lymph node only, and **N2/3** involvement of post-sentinel lymph nodes.

Supplementary figure 10

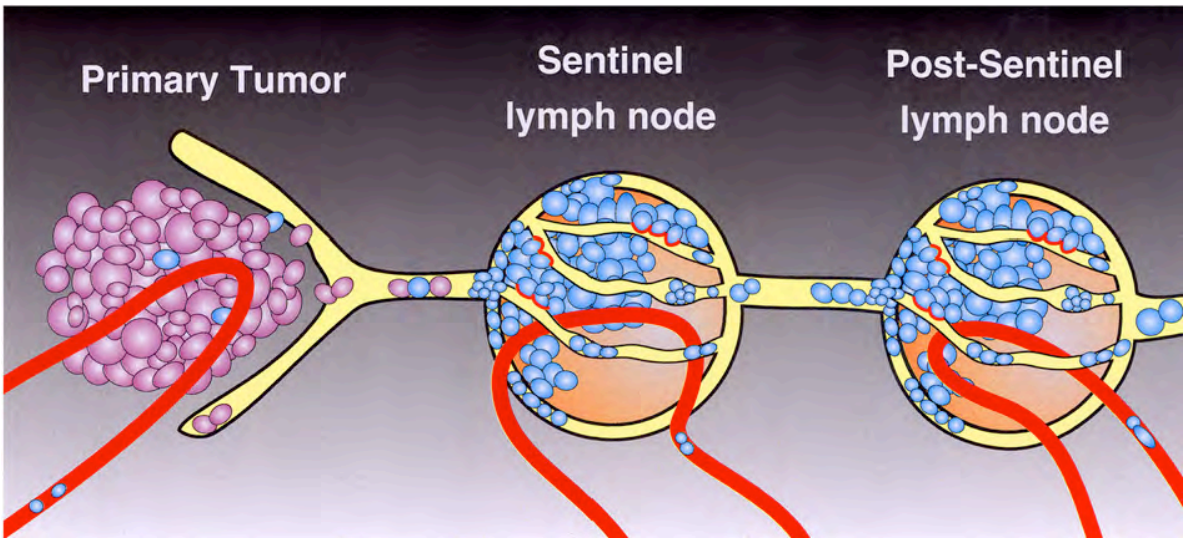

Figure 10, Metastatic spreading of carcinoma cells (blue) from the primary tumors **(left)** to the sentinel (**center**) and post-sentinel (**right**) lymph nodes. **Primary tumors:** lymphatic vessels (**yellow**) surround the tumors, and are invaded by detached potentially metastatic tumors cells (peritumoral carcinosis). Blue tumor cell clones express lymphangiogenic factors.**Sentinel lymph node**: a pre-metastatic niche is formed by expansion of lymph node sinus and conversion of their lining cells into lymphatic endothelial cells ("lymph node lymphangiogenesis"). Intrametastatic lymphatic vessels are invaded by tumors cells (**red caps on tumors cells**) from the metastatic colony, and tumor emboli in the lymphatic vessels migrate towards the subsequent lymph nodes. **Post-sentinel lymph node(s):** Repetition of events in the sentinel lymph nodes. It is currently not clear if tumor cells enter bdod vessels (**red**) in primary or metastatic tumors.

Supplementary Video

Migration of lymphatic endothelial cells beneath a MCF7 cell spheroid

A monolayer of Cytotracker green tagged lymphatic endothelial cells was grown to confluence, and a MCF-7 cells spheroid was placed on top. The frames were taken in 15 min intervals, the total time of the video comprises 240 min.